

Penta-Hepta Defect Motion in Hexagonal Patterns

Lev S. Tsimring

Institute for Nonlinear Science, University of California, San Diego, California 92093-0402

(Received 3 January 1995)

The structure and dynamics of penta-hepta defects (PHD's) in hexagonal patterns are studied in the framework of coupled amplitude equations for the underlying plane waves. An analytical solution for the phase field of moving PHD is found in the far field, which generalizes the static solution due to Pismen and Nepomnyashchy. The mobility tensor of the PHD is calculated using a combined analytical and numerical approach. The results for the velocity of a PHD climbing in slightly nonoptimal hexagonal patterns are compared with numerical simulations of amplitude equations. The interaction of penta-hepta defects in optimal hexagonal patterns is considered.

PACS numbers: 47.20.Ky, 47.27.Te, 64.90.+b

Hexagonal patterns in nonequilibrium extended systems are formed as a result of superposition of three plane waves oriented at 120° with respect to each other. They appear naturally in a large variety of pattern-forming systems in fluid dynamics, optics, chemical kinetics, etc. [1]. The most generic defect in hexagonal patterns is the so called penta-hepta defect (PHD) which is a bound state of two dislocations of opposite winding numbers on two different wave systems [2]. In the paper [3] we have demonstrated that the mechanism which provides the binding force is the synchronization of the phase fields in the bulk of the system so the resonant condition for phases can be fulfilled everywhere except at the core of the defect. If the wave numbers of waves composing the hexagonal pattern are equal to the onset value of cellular instability, the PHD stays put. Meanwhile, observations of penta-hepta defects in non-Boussinesq Rayleigh-Bénard convection and in other systems demonstrate that PHD's in fact move slowly and eventually annihilate or disappear at the boundaries [4]. It is conceivable that the motion of PHD's is caused by the ambient strain due to the deviation of the wave numbers from the onset value (and thus provides a wave number selection mechanism), or by defect interaction with each other. An example of a nonoptimal hexagonal pattern, nonequilateral (rhombic) hexagons, was considered recently in a number of papers [5,6]. As we shall see, even equilateral hexagonal patterns with wave numbers different from the optimal value produce the driving Peach-Köhler force for a penta-hepta defect. These nonoptimal equilateral pattern were considered in [7-9].

In this Letter, the motion of PHD's in nonoptimal hexagonal patterns is considered. The analysis is carried out in the framework of three coupled equations for the complex amplitudes of individual waves. These equations constitute the simplest heuristic model for hexagonal patterns and play essentially the same role here as the complex Ginzburg-Landau equation for oscillatory media or the Newell-Whitehead-Segel equation for roll patterns in isotropic media.

The order parameter of the hexagonal pattern is written in the form $a = \epsilon^{1/2} \sum_{j=1}^3 B_j \exp[i(\mathbf{k}_j + \mathbf{K}_j)\mathbf{r}] + \text{c.c.}$,

where ϵ is a small parameter characterizing the distance above onset, all three $|\mathbf{k}_j| = k_0$, the onset wave number of the symmetry-breaking instability, \mathbf{k}_1 , points in the x direction (polar angle $\phi = 0$), and $\mathbf{k}_{2,3}$ point at $\phi = \pm 2\pi/3$, respectively. \mathbf{K}_j are rescaled corrections to the optimal wave vectors \mathbf{k}_j , $\sum_{j=1}^3 \mathbf{K}_j = 0$ from the resonance condition. The complex amplitudes B_j are slow functions of $\mathbf{R} = \epsilon^{1/2}\mathbf{r}$ and $T = \epsilon t$. B_j satisfy the following triplet of equations [8]:

$$\begin{aligned} \partial_T B_j = & (\mu - K_j^2) B_j + B_{j-1}^* B_{j+1}^* - (|B_j|^2 + \gamma |B_{j-1}|^2 \\ & + \gamma |B_{j+1}|^2) B_j + (\mathbf{n}_j \cdot \nabla)^2 B_j + 2i K_j (\mathbf{n}_j \cdot \nabla) B_j. \end{aligned} \quad (1)$$

Here \mathbf{n}_j is the unit vector oriented along the wave vector of wave j , $\mathbf{n}_1 = (1, 0)$, $\mathbf{n}_2 = (-\frac{1}{2}, \frac{\sqrt{3}}{2})$, $\mathbf{n}_3 = (-\frac{1}{2}, -\frac{\sqrt{3}}{2})$, index j is defined modulo 3, the coefficient of quadratic nonlinearity is rescaled to unity, μ is the rescaled supercriticality parameter, γ is the ratio of the coefficient of cubic interaction of different orientation to the coefficient of cubic self-interaction, and $K_j = (\mathbf{n}_j \cdot \mathbf{K}_j)$. Spatial gradients are calculated with respect to the slow variable \mathbf{R} , and asterisks denote the complex conjugate. The applicability of these equations to the description of real hexagonal patterns has been discussed earlier [3,8,10].

Equations (1) have a family of uniform stationary solutions, B_j^0 , of which only the equilateral one ($K_j = K$) can be expressed in a simple analytic form,

$$B_j^0 = B_0 = \frac{1 + \sqrt{1 + 4(\mu - K^2)(1 + 2\gamma)}}{2(1 + 2\gamma)}. \quad (2)$$

In the general case of different K_j the amplitudes B_j are different, and the solutions are known as rhombic patterns.

Spontaneously formed hexagonal patterns are usually defect ridden. Various defects have been described in the literature (see, for example, [11]). Most of them are not stable and either disappear quickly or transform into basic penta-hepta defects. A PHD is a bound state in which two of the three modes have dislocations with opposite winding numbers. Without loss of generality we will consider a particular form of penta-hepta defect with

positive dislocation in mode 2 and negative dislocation in mode 3. Mode 1 contains no dislocations. The corresponding static solution to (1) with $K_j = 0$ can be written in the form $A_j = F_j(R, \phi) e^{i\theta_j(R, \phi)}$, where R and ϕ are polar coordinates, $\oint_C \nabla \theta_1 ds = 0$, $\oint_C \nabla \theta_{2,3} ds = \pm 2\pi$, $F_{1,2}(0) = 0$, $F_{1-3}(\infty) = B_0$, and C is a closed contour encircling the origin. This solution cannot be expressed in a closed analytic form. However, in the far field where all the amplitudes approach the asymptotic value B_0 , the following solution for the phase fields θ_j depending only on the polar angle ϕ has been found [10],

$$\begin{aligned} \theta_1 &= (1 - \cos 2\phi) \frac{\sqrt{3}}{6}, \\ \theta_{2,3} &= \pm \phi - \left[\frac{1}{2} - \cos\left(2\phi \mp \frac{2\pi}{3}\right) \right] \frac{\sqrt{3}}{6}. \end{aligned} \quad (3)$$

In order to find the equations of motion for the penta-hepta defect in the nonoptimal hexagonal pattern, we assume that the PHD moves with a constant velocity \mathbf{V} . Transforming into a moving frame $\mathbf{R}' = \mathbf{R} - \mathbf{V}T$ then yields the set of stationary equations for $B_j(\mathbf{R}')$ which coincides with (1) with ∂_T replaced by $-\mathbf{V}\nabla B_j$. Then we project these equations onto their two orthogonal translational modes $\{\partial_\xi^* B_j\}$ and $\{\partial_\eta^* B_j\}$ [we choose a new coordinate frame (ξ, η) where $\xi = X \cos \psi + Y \sin \psi$ is the coordinate along the defect motion, $\eta = Y \sin \psi - X \cos \psi$ orthogonal to that, and ψ is the angle between the direction of defect motion and the X axis]:

$$\bar{\mathbf{T}} \cdot \mathbf{V} \equiv \begin{pmatrix} I_{\xi\xi} & I_{\xi\eta} \\ I_{\eta\xi} & I_{\eta\eta} \end{pmatrix} \begin{pmatrix} V \\ 0 \end{pmatrix} = \begin{pmatrix} T_1 \\ T_2 \end{pmatrix}, \quad (4)$$

where $\bar{\mathbf{T}}$ is the mobility tensor of the PHD,

$$\begin{aligned} I_{\xi\xi} &= \left\langle \sum_{j=1}^3 |\partial_\xi B_j|^2 \right\rangle, & I_{\eta\eta} &= \left\langle \sum_{j=1}^3 |\partial_\eta B_j|^2 \right\rangle, \\ I_{\xi\eta} &= I_{\eta\xi} = \frac{1}{2} \left\langle \sum_{j=1}^3 \partial_\xi B_j \partial_\eta B_j^* + \text{c.c.} \right\rangle, \\ T_1 &= 2\pi [|B_2^0|^2 K_2 \sin(\psi - 2\pi/3) \\ &\quad - |B_3^0|^2 K_3 \sin(\psi + 2\pi/3)], \\ T_2 &= 2\pi [|B_2^0|^2 K_2 \cos(\psi - 2\pi/3) \\ &\quad - |B_3^0|^2 K_3 \cos(\psi + 2\pi/3)]. \end{aligned}$$

and $\langle \dots \rangle = \iint \dots dXdY$. All other terms from the right-hand side (RHS) of Eq. (1) vanish upon integration under the usual boundary conditions at infinity. Here we used the formula

$$\langle \partial_X B_j \partial_Y B_j^* \rangle - \text{c.c.} = 2\pi i \delta_j |B_j^0|^2, \quad (6)$$

where δ_j is the winding number of the dislocation at the particular mode, $\delta_1 = 0$ and $\delta_{2,3} = \pm 1$, respectively.

Equations of motion (4) indicate that the penta-hepta defect is driven by superposition of two Peach-Köhler forces corresponding to a strain at singular modes 2,3. If $K_{2,3} = 0$, the defect does not move. The strain at the nonsingular mode 1 does not enter explicitly into the equations (4); however, implicitly K_1 affects the amplitudes B_j^0 .

The well known difficulty in treating equations of motions for topological defects is that integrals entering their mobilities diverge. Indeed, with the static phase approximation solution (3) components of $\bar{\mathbf{T}}$ diverge logarithmically at both small and large R . At small R the phase approximation is not valid, and the stationary solution of the full amplitude Eqs. (1) should be employed. A more serious problem arises at large R . Evidently, one could introduce an *ad hoc* large-scale cutoff due to finite-size effects, and therefore the mobility will be logarithmically dependent on the size of the box. This may be relevant only for small systems ($VR_{\text{box}} \ll 1$). Another possibility considered in the literature [12,13] for regular dislocations is to use solutions corresponding to moving defects. In this case the integrals converge and therefore a finite velocity of dislocations can be found even in the large box limit ($VR_{\text{box}} \gg 1$). In the spirit of the calculation scheme [13] we assume that all K_j are small, therefore the velocity of the PHD is also small, and the solution describing moving defect differs from the stationary one only at large distances $R \sim V^{-1} \gg 1$, where the phase approximation is well justified. Therefore the region of integration for the components of the mobility tensor can be split into two parts; in the inner region ($R < R_0$, where $1 \ll R_0 \ll |V|^{-1}$) the stationary PHD solution can be used, and in the outer region ($R > R_0$) the phase approximation can be used to simplify the task of finding the moving PHD solution. At $R \sim R_0$ the static phase approximation solution (3) is applicable, so both parts should depend on R_0 logarithmically. After adding them together the radius R_0 should drop out.

The details of this rather involved calculation will be published elsewhere [14]. The final expressions for the mobility components are relatively simple,

$$\begin{aligned} I_{\xi\xi} &= -B_0^2 [(5\pi/2) \ln(w_1 V) - \pi \cos 2\psi \ln(w_2 V)] \\ I_{\xi\eta} &= B_0^2 \pi \sin 2\psi \ln(w_3 V), \end{aligned} \quad (7)$$

where $w_1 = 1.24$, $w_2 = 1.14$, and $w_3 = 2.00$ (we do not need $I_{\eta\eta}$).

Now we can substitute (5) and (7) into (4). Since we already assumed all three K_j small, without further loss of accuracy we can take in (5) all three $|B_j| = B_0$, after which it is canceled. Thus we obtain a set of two nonlinear algebraic equations for V and ψ ,

$$\begin{aligned} \frac{5}{2} V \ln(w_1 V) + V \ln(w_2 V) \cos 2\psi &= 2K_2 \sin(-\psi + 2\pi/3) + 2K_3 \sin(\psi + 2\pi/3), \\ V \ln(w_3 V) \sin 2\psi &= 2K_2 \cos(-\psi + 2\pi/3) - 2K_3 \cos(\psi + 2\pi/3). \end{aligned} \quad (8)$$

In these equations there are only three $O(1)$ constants which (for small K_j) are functions of the parameters μ and γ only.

Equations (4) have been written for a particular penta-hepta defect with positive dislocation in mode 2, negative dislocation in mode 3, and no dislocation in mode 1. We label it as $(0, 1, -1)$. Totally, there exist six distinct penta-hepta defects, $(0, 1, -1)$, $(1, 0, -1)$, and $(1, -1, 0)$, and their mirror images (conjugate defects) $(0, -1, 1)$, $(-1, 0, 1)$, and $(-1, 1, 0)$. The equations for $(1, 0, -1)$ and $(1, -1, 0)$ PHD's can be obtained from Eqs. (8) by the cyclic relabeling of $K_{1,2,3}$ and replacing ψ by $\psi \pm 2\pi/3$. For a conjugate PHD, the mobility tensor remains the same, but the RHS of the equations of motion changes sign. Obviously, for conjugate defects, $V^* = V$ and $\psi^* = \psi + \pi$.

Numerical simulations of the amplitude equations (1) were performed using a split-step pseudospectral method. Typically we used 256^2 spatial harmonics with periodic boundary conditions. We used two physical system sizes $L = 100$ and 40 to check the importance of finite-size effects, and the time step was chosen as 0.1 . To diminish the effect of periodic boundary conditions we introduce a circular ramp at $R > 0.4L$. In all examples described below $\mu = 1$, $\gamma = 2$. As the initial condition we take a static $(0, 1, -1)$ defect placed in the middle of the integration domain.

In Fig. 1 the magnitude and angle of the velocity vector found from (4) are plotted together with the results of direct numerical simulations versus K_3 for $K_1 = K_2 = 0.1$. Quantitative comparison indicates that both the direction

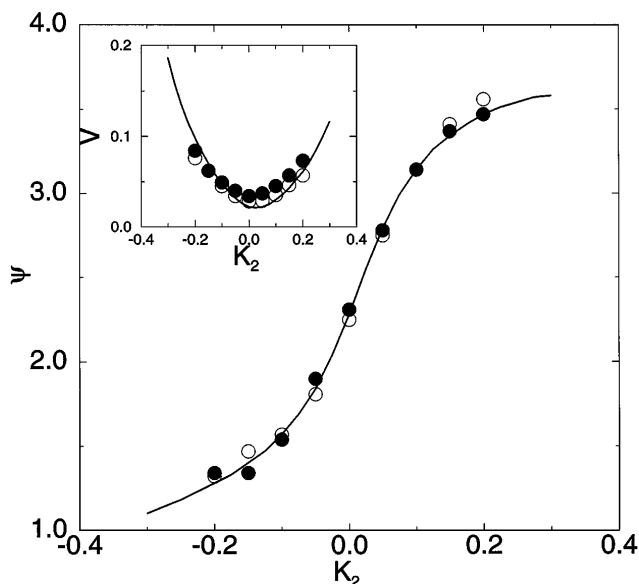


FIG. 1. Velocity vector of a PHD $(0, 1, -1)$ as a function of wave number correction K_2 at $K_1 = 0.1$, $K_3 = 0.1$. Main panel: angle with respect to the X axis, parameters $\mu = 1$, $\gamma = 2$; inset: magnitude. Solid lines: theory, Eqs. (8); open circles: numerical simulations of (1) with system size $L = 40$; solid circles: same for $L = 100$.

of motion and the magnitude of the velocity are in a good agreement with the theoretical analysis. Numerical calculations confirm that the direction of PHD motion strongly depends on the combination of the wave number corrections at the singular modes. Wave number detuning at the nonsingular mode K_1 only weakly affects \mathbf{V} via the amplitudes B_j^0 . Notably, even if all three wave vectors are equal (but nonoptimal), the PHD still moves along the X axis (the wave vector of the nonsingular mode).

It is tempting to apply the equations of motion (8) directly to the interaction of two PHD's. Indeed, when two PHD's are far enough apart, they interact entirely through phase perturbations. Each defect distorts the phase field and therefore creates a slightly nonoptimal hexagonal pattern at the location of another defect. However, if we assume that the field is static, and estimate the convergence velocity for a distance R , we obtain $VR \approx 2$ which clearly is inconsistent with this assumption. Strictly speaking, the phase field "remembers" the whole previous path of the defects, and therefore Eqs. (8) can give only qualitative predictions for the defect interaction.

Here we present some of the results of numerical simulations of interacting penta-hepta defects in an ideal (all $K_j = 0$) pattern. The result of interaction (attraction or repulsion) of two PHD's $(\delta_1^1, \delta_2^1, \delta_3^1)$ and $(\delta_1^2, \delta_2^2, \delta_3^2)$ depends on the number $N = \sum_{j=1}^3 \delta_j^1 \delta_j^2$. It can only take values of $-2, -1, 1$, and 2 . If $N < 0$ defects are attracted, and in other cases they repel each other. In Figs. 2(a) and 2(b) two families of PHD trajectories are shown for several initial positions of defects. Figure 2(a) illustrates the attraction of two conjugate defects, $(0, 1, -1)$ and $(0, -1, 1)$ (in this case $N = -2$ and defects are attracted). After collision pairs of dislocations at modes 2 and 3 annihilate, and thus a perfect hexagonal pattern is established. Meanwhile, two PHD's of the same type $(0, 1, -1)$ (here $N = 2$) repel each other [see Fig. 2(b)]. For two different PHD's $(0, 1, -1)$ and $(-1, 0, 1)$, $N = -1$, and the defects are attracted again; however, complete annihilation does not occur. Instead, conjugate dislocations at mode 3 annihilate, and the remaining dislocations at modes 2 (from the first PHD) and 1 (from the second PHD) immediately form a

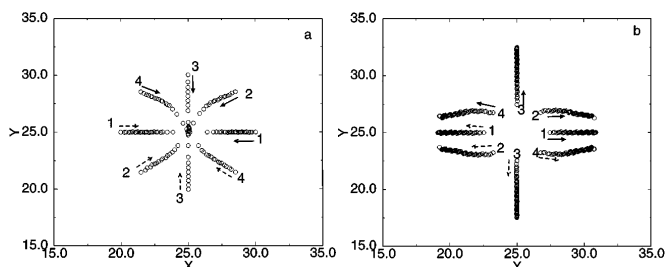


FIG. 2. Trajectories of interacting penta-hepta defects. Open circles indicate positions of the defect cores with time interval $\Delta T = 2.5$. Arrows point toward directions of motion; (a): $(0, 1, -1)$ (solid) and $(0, -1, 1)$ (dashed); (b): $(0, 1, -1)$ and $(0, 1, -1)$. For each case, four sets of initial conditions are taken (they are labeled 1-4 in the figures).

new penta-hepta defect $(-1, 1, 0)$. As this defect is alone, and the ambient strain is absent, the defect stays put.

In Fig. 3(a) the distance between the two cores is shown as a function of time for interacting $(0, 1, -1)$ and $(0, -1, 1)$ defects. The rate of convergence varies with the initial positions of the defects. Attraction is strongest for defects aligned along the Y axis, and weakest for defects aligned along X axis. Figure 3(b) plots the same data in logarithmic coordinates. Rather unexpectedly, one can see that over large time intervals the data are consistent with $R \propto (T_c - T)^{1/2}$ law, which in turn suggests $V \propto R^{-1}$ scaling. Up to logarithmic corrections this scaling is what one could expect in the static approximation discussed above. The same scaling is observed for other PHD configurations.

We investigated the motion of penta-hepta defects in slightly nonoptimal hexagonal patterns and their interaction. It follows from our results that PHD's provide an important mechanism for wave number selection in hexagonal patterns, similar to dislocations in roll patterns. PHD is stationary only in the perfect pattern with wave numbers of all three modes equal to the onset value (in hexagonal patterns it does not correspond to the boundary of zig-zag instability) [15]. In nonoptimal hexagonal patterns a PHD is driven by the superposition of two Peach-Köhler forces, corresponding to two singular modes. PHD's attract or repel each other depending on the parameter N introduced above. The trajectories of interacting defects may be rather complicated. Furthermore, when two attracting PHD's collide, they do not necessarily annihilate, but may give rise to another PHD with a different topological structure.

Equations (1) represent the simplest possible model for hexagonal pattern formation. Nevertheless, it captures most generic features of real hexagonal patterns. We believe that detailed experiments with thermoconvection or parametric ripples similar to ones which have been performed for dislocations in roll patterns [16] could test the predictions of our theory. More realistic models

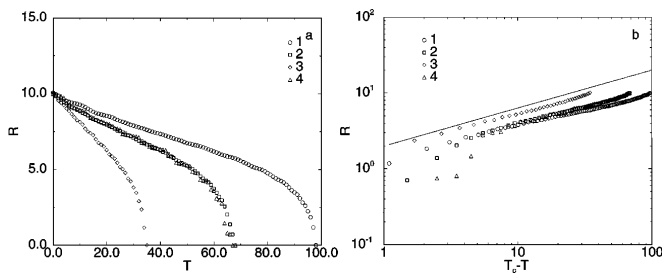


FIG. 3. Distances between interacting penta-hepta defects $(0, 1, -1)$ and $(0, -1, 1)$ versus time. (a): linear coordinates; (b): logarithmic coordinates. Labels 1–4 correspond to different initial positions of the defects, as shown in Fig. 2(a). The straight line indicates the $R \sim T^{-1/2}$ law.

usually include nonvariational terms (see, e.g., [6]). When these terms are not small (usually far from threshold), they can affect the defect dynamics significantly, for example, lead to the spontaneous nucleation of defects and complex spatiotemporal behavior known as defect chaos.

Author is grateful to I. Aranson, H. Levine, and M. I. Rabinovich for useful discussions. This work was supported by the U.S. Department of Energy under Contract No. DE-FG03-90ER14138 and by the Office of Naval Research under Contract No. N00014-D-0142 DO#15.

-
- [1] E. Bodenschatz, J.R. DeBruyn, G. Ahlers, and D.S. Cannell, *Phys. Rev. Lett.* **67**, 3078 (1991); W.J. Firth, *Proc. SPIE Int. Soc. Opt. Eng. (U.S.A.)* **2039**, 290 (1993); Q. Ouyang, and H.L. Swinney, *Nature (London)* **352**, 61 (1991).
 - [2] S. Ciliberto, P. Coulet, J. Lega, E. Pampaloni, and C. Perez-Garcia, *Phys. Rev. Lett.* **65**, 2370 (1990).
 - [3] M. I. Rabinovich and L. S. Tsimring, *Phys. Rev. E* **49**, R35 (1993).
 - [4] G. Ahlers (private communication).
 - [5] Q. Ouyang, G. H. Gunaratne, and H. L. Swinney, *Chaos* **3**, 707 (1993); B. A. Malomed, A. A. Nepomnyashchy, and A. E. Nuz, *Physica (Amsterdam)* **70D**, 357 (1994).
 - [6] E. A. Kuznetsov, A. A. Nepomnyashchy, and L. M. Pismen, *Technion Report*, 1994 (to be published).
 - [7] B. A. Malomed and M. I. Tribelsky, *Sov. Phys. JETP* **65**, 305 (1987).
 - [8] M. M. Sushchik and L. S. Tsimring, *Physica (Amsterdam)*, **74D**, 90 (1994).
 - [9] J. Lauzeral, S. Metens, and D. Walgraef, *Europhys. Lett.* **24**, 707 (1993).
 - [10] L. M. Pismen and A. A. Nepomnyashchy, *Europhys. Lett.* **24**, 461 (1993).
 - [11] J. Pantaloni and P. Cerisier, in *Cellular Structures in Instabilities*, edited by J.E. Weisfreid and S. Zaleski (Springer-Verlag, Berlin, 1984).
 - [12] E. D. Siggia and A. Zippelius, *Phys. Rev. A* **24**, 1036 (1981); Y. Pomeau, P. Manneville, and S. Zaleski, *Phys. Rev. A* **27**, 2710 (1983); G. Tesauro and M. C. Cross, *Phys. Rev. A* **34**, 1363 (1986).
 - [13] E. Bodenschatz, W. Pesch, and L. Kramer, *Physica (Amsterdam)* **32D**, 135 (1988).
 - [14] L. S. Tsimring (to be published).
 - [15] Far from threshold, wave number selection becomes imperfect, as PHD's can be trapped by an underlying cellular structure. This is why in our opinion static dislocation densities were observed in some experiments [11].
 - [16] A. Pocheau and V. Croquette, *J. Phys* **45**, 35 (1984); R. Ribotta and A. Joets, in *Cellular Structures in Instabilities* (Ref. [11]), p. 249.